Numerical Analysis of Cahn-Hillard Equation with Runge-Kutta Methods

Jeremiah Coleman[1]

[1]APC 523 Final Project

Abstract

Understanding the dynamics behind the disorder in various material systems is crucial for optimizing a material's chemicals and physical properties. A common method of developing highly disordered materials is via a process called spinodal decomposition. Spinodal decomposition is the process at which two or more components of a mixture rapidly separate under specific conditions into distinct phases with different chemical compositions and physical properties. The dynamics of this decomposition is governed the Cahn-Hillard equation, a modified diffusion equation $\frac{\partial \mathbf{c}}{\partial t}(\mathbf{x}, t) = \nabla \cdot [M(\mathbf{c}) \cdot \nabla \mu(\mathbf{c})]$ where $\mathbf{c}(\mathbf{x}, t)$ represents the phase field defined as the fraction of one of the binary mixtures. Other variables correspond to the free energy of the system and mobility of the material. In this work we will demonstrate the advantages and disadvantage of the family of Runge-Kutta numerical schemes for analyzing simple iterations of this stiff-nonlinear parabolic PDE. We will assume a central difference spatial discretization and analyze the stability and symplectic nature of each scheme. We conclude this work with the results of our schemes and methodologies for expanding to more complex situations such as complex geometries and spatially dependent parameters.

1. Introduction

Spinodal decomposition is a phase transformation by which initially a homogeneous mixture spontaneously separates into islands rich in one component and matrix rich in another component. The Cahn-Hillard equation is formally a stiff, fourth-order, non-linear parabolic partial differential equation that was initially derived to model such phase separation in binary alloy systems. It now has applications in other applications throughout engineering including image inpainting, multiphase fluid dynamics, tumour growth and topology optimization (Amiri et al., 2019; Valizadeh & Rabczuk, 2019; Zimmermann et al., 2019). The equation most generally takes the following form:

$$\frac{\partial \mathbf{c}}{\partial t}(\mathbf{x}, t) = \nabla \cdot [M(\mathbf{c}) \cdot \nabla \mu(\mathbf{c})], \quad \mathbf{c} \in \Omega, \ t > 0 \tag{1}$$

where $\mathbf{x}$ is the position vector, Ω is the domain, $\mathbf{c}(\mathbf{x}, t)$ is the mass concentration, $M(\mathbf{c})$ is a mobility function related to the mobility of the species, and $\mu(\mathbf{c})$ is the chemical potential. Generally periodic Neumann boundary conditions are applied to resemble the effects of bulk decomposition, but Direchelot can be used to model realistic boundary affects. Figure [1] demonstrates a sample simulation of the spinodal decomposition of a binary system in 2-D governed by the Cahn-Hillard equation.

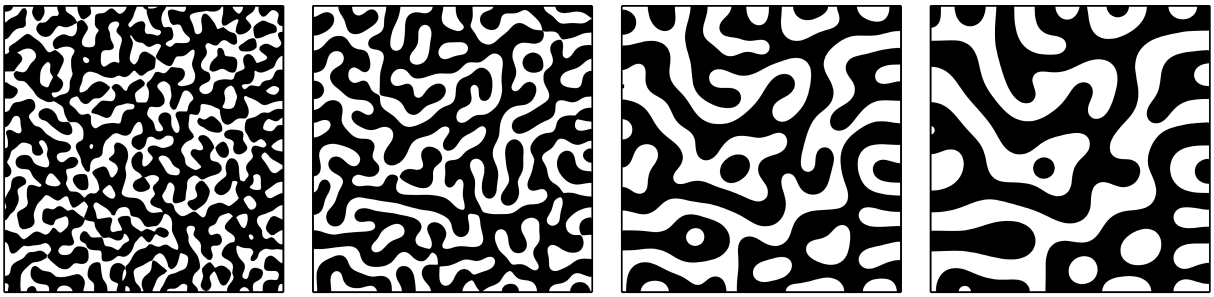

Figure 1: Sample simulation of spinodal decomposition governed by the modified Cahn-Hillard equation from Shin et al., 2019

As will be discussed more in Section 2, the dynamics of the Cahn-Hillard equation is determined by the functional form of the chemical potential μ. For chemical potentials with double-well local energy functionals, the Cahn-Hillard equation describes the, simultaneous, fast phase separation between two phases and slow coarsening leading to bulk phases with interfaces separating them. These two processes are characterized by different time and space scales, making it difficult to solve accurately and efficiently in feasible time limits and using reasonable computational resources.

We start off in Section 2 deriving the modified Cahn-Hillard equation that governs spindoal decomposition, derive the the chemical potential functional form we will analyze, and introduce the decreasing total energy of the system. In Section 3, we will introduce the family of Runge-Kutta methods used to simulate the modified Cahn-Hillard equation. We will discuss their spatial and temporal discretization, stability and ability to conserve the total energy. These methods include Forward and Backward Euler, The Runge Kutta method, and a 5 stage ESDIRK. In Section 4 we will analyze the results of the various numerical methods. Finally in Section 5 we will discuss how to add various complexities to the model, such as spatial mobility and realistic boundary conditions through different geometries.

2. Background & Derivation

Without delving into the fundamentals of material energy systems, we will derive the Cahn-Hillard equation to demonstrate intuition for the dynamics of the evolution and what parameters are realistically tunable for spinodal decomposition. Spinodal decomposition is a phase transition between an initial binary homogeneous mixture that spon-

taneously separates into islands rich in one component and a matrix rich in the other. Due to the increase energy associated with interferances between the binary components, the Cahn-Hillard equation describes how the system evolves to reduce the energy in the system by searching for equilibrium concentrations and reducing the interfaces.

We consider a binary mixture of two components A and B described by a molar concentration $c_A(\mathbf{x}, t)$ and $c_B(\mathbf{x}, t)$ respectively where $\mathbf{x}$ is the position vector. Since we assume the system is closed, the total concentration is constant thus $c_A(\mathbf{x}, t)+c_B(\mathbf{x}, t) = 1$. Due to this relationship, we only need to evolve one component to keep track of the system. Thus we define:

$$c(\mathbf{x}, t) = c_A(\mathbf{x}, t) \tag{2}$$

$$c_B(\mathbf{x}, t) = 1 - c(\mathbf{x}, t) \tag{3}$$

Frick's first Law states the diffusive flux of a component is driven by the gradient of the concentration at every point. Classical thermodynamics states that for a conservative (isolated) system, the chemical potential drives configurational change to minimize the energy of the system. Thus:

$$J = -M(\mathbf{x}, t) \cdot \nabla\mu(\mathbf{c}, t) \tag{4}$$

where $M(\mathbf{x}, c)$ is the mobility coefficient and $\mu(\mathbf{c}, t)$ is the chemical potential. Specifically, the chemical potential quantifies how much the energy changes with respect to the concentration, $\mu(\mathbf{c}, t) = \frac{\partial E(\mathbf{c},t)}{\partial c}$, where $E(\mathbf{c}, t)$ is the energy of the system. Assuming conservation of mass, the *Cahn-Hillard equation* comes from the continuity equation

$$0 = \frac{\partial \mathbf{c}}{\partial t}(\mathbf{x}, t) + \nabla J \tag{5}$$

$$= \frac{\partial \mathbf{c}}{\partial t}(\mathbf{x}, t) - \nabla(M(\mathbf{x}, t) \cdot \nabla\mu(\mathbf{c}, t) \tag{6}$$

$$= \frac{\partial \mathbf{c}}{\partial t}(\mathbf{x}, t) - \nabla \left(M(\mathbf{x}, t) \cdot \nabla \frac{\partial E(\mathbf{c}, t)}{\partial \mathbf{c}} \right) \tag{7}$$

$$\tag{8}$$

The total Gibbs free energy $E(\mathbf{c}, t)$ for an isotropic system is defined as

$$E(\mathbf{c}, t) = \int_\Omega \frac{\kappa}{2}|\nabla \mathbf{c}|^2 + f(\mathbf{c}, t)d\mathbf{x} \tag{9}$$

where $f(\mathbf{c}, t)$ is the free energy per molecule for a given system and κ is a constant called gradient energy coefficient. The first term represents the energy of the homogeneous parts of the system while the second term represents the interracial energy of the system.

From this we arrive at the modified Cahn-Hillard equation

$$0 = \frac{\partial \mathbf{c}}{\partial t}(\mathbf{x}, t) - \nabla \left(M(\mathbf{x}, t) \cdot \nabla \frac{\partial E(\mathbf{c}, t)}{\partial c} \right) \tag{10}$$

$$0 = \frac{\partial \mathbf{c}}{\partial t}(\mathbf{x}, t) - \nabla \left(M(\mathbf{x}, t) \cdot \nabla \left(-\kappa \nabla^2 \mathbf{c} + \frac{df(\mathbf{c}, t)}{d\mathbf{c}} \right) \right) \tag{11}$$

$$\frac{\partial \mathbf{c}}{\partial t}(\mathbf{x}, t) = \nabla \left(M(\mathbf{x}, t) \cdot \nabla \left(\frac{\partial f(\mathbf{c}, t)}{\partial \mathbf{c}} - \kappa \nabla^2 c \right) \right) \tag{12}$$

The problem statement can also be expressed as

$$\frac{\partial \mathbf{c}}{\partial t}(\mathbf{x}, t) = \nabla (M(\mathbf{x}, t) \cdot \nabla \mu(\mathbf{c}, t))$$
$$\mu(\mathbf{c}, t) = b\mathbf{c}^3 + a\mathbf{c} - \kappa \nabla^2 \mathbf{c}$$

We refer to this equation as the *modified Cahn-Hillard equation.* The kinetics of phase separation and coarsening is described by this modified Cahn–Hilliard equation. It describes how the total energy of the system is dissipated in the conservative system, conserving the mass of the system while minimizing the total energy.

2.1 Intuition from Total Energy of the System

The dynamics of the system is to minimize the total energy of the system

$$E(\mathbf{c}, t) = \int_\Omega \frac{\kappa}{2} |\nabla \mathbf{c}|^2 + f(\mathbf{c}, t) d\mathbf{x}. \tag{13}$$

Thus the dynamics will reach an equilibrium that minimizes $f(\mathbf{c})$ and $\nabla \mathbf{c}$. For the former, after a short time the system will be at a singular (or multiple) $\mathbf{c}_{min}$ where $\partial f_c(\mathbf{c}_{min}) = 0$. For the latter, the system will slowly reduce the boundaries between these minima regions by merging smaller regions of same concentration to larger regions ie reducing the number of boundaries. This process is called **coarsening**.

While $f(\mathbf{c})$ can take any arbitrary function, spinodal decomposition occurs when $f(c)$ has two minima corresponding to the equilibrium concentrations. Thus we will assume the following convex double well functional

$$f(\mathbf{c}, t) = \frac{a(t)\mathbf{c}^2}{2} + \frac{b(t)\mathbf{c}^4}{4} \tag{14}$$

where a, b are constants. Figure 2 shows the general forms of the functional depending on the relevant constant a, b which determines whether the functional is a double well or single well potential or convex vs concave.

This functional $f(\mathbf{c})$ is a common approximation of binary systems which generally

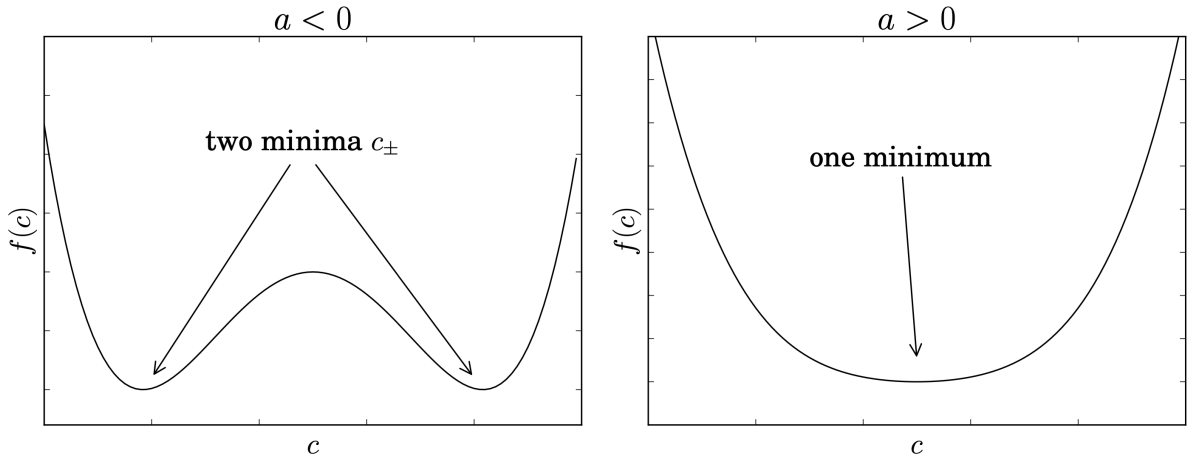

Figure 2: Approximation function of local free energy $f(\mathbf{c})$ of a binary mixture. Generally there is a critical temperature that determines the sign of a and thus whether the system undergoes spinodal decomposition or not. b is assumed to be positive.

take on the form

$$f(\mathbf{c}, t) = A(t)[\mathbf{c} \ln \mathbf{c} + (1 - \mathbf{c}) \ln(1 - \mathbf{c})] + B(t)\mathbf{c}(1 - \mathbf{c}). \tag{15}$$

where $A(t), B(t)$ are related to external parameters such as temperature and pressure.

If we assume $a(t) = a_0 < 0, b(t) = b_0 > 0$ to ensure the functional is double-well and convex, and $M(\mathbf{c}, t) = M_0$, then the problem statement becomes

$$\begin{aligned} \frac{\partial \mathbf{c}}{\partial t}(\mathbf{x}, t) &= \nabla(M_0(\mathbf{x}, t) \cdot \nabla \mu(\mathbf{c}, t)) \\ \mu(\mathbf{c}, t) &= b\mathbf{c}^3 + a\mathbf{c} - \kappa \nabla^2 \mathbf{c} \end{aligned}$$

known as the *simple* modified Cahn-Hillard equation. We will have $b = -a$ so then the local minima of f are at $c = \pm 1$. Thus $\mathbf{c} = +1$ corresponds to component A and $\mathbf{c} = -1$ corresponds to component B.

Due to the conserved energy quantity existing, we want symplectic numerical schemes that inherit this energy conserving property as well. While analyzing the following numerical methods, we will use the energy system to determine the accuracy of the solution.

3. Runge-Kutta Methods for Simple Modified Cahn-Hillard Equation

The Runge-Kutta methods are a family of implicit and explicit, iterative multi-stage numerical schemes with respect to temporal discretization. We will evaluate the simple modified Cahn-Hillard equation with the one stage explicit scheme (Forward Euler), the four-stage explicit scheme, one stage implicit scheme (Backward Euler), and a single

diagonal implicit scheme. We will include linearization, non-linear solvers and adaptive time measurements. For the spatial discretization we will use 2nd order finite difference. We will demonstrate the limitations of explicit schemes due to the stiffness of the equation requiring implicit schemes which can be computationally costly but more flexible.

We will assume initially periodic Neumann boundary conditions to mimic simulation of the bulk of the system system.

$$\frac{\partial c(\mathbf{x},t)}{\partial n} = \frac{\partial \mu(\mathbf{x},t)}{\partial n} = 0,\ \mathbf{x} \in \partial\Omega \tag{16}$$

where $\partial\Omega$ represents the boundary and n is the outward normal derivative at the domain boundary. For this section we will focus on a 2D domain.

3.1 Spatial Discretization

Let Ω be the planar domain $[0,1]$. Lets consider a uniform mesh of N x N cells over Ω leading to a mesh size of $h = 1/N$.

3.1.1 Finite Difference Scheme

One method to spatially discrete the problem is a simple 2nd order central finite difference scheme of the second and fourth order derivative operators in 12. The problem can be written with the following discrete operators

$$\frac{\partial \mathbf{c}}{\partial t}(\mathbf{x},t) = M_0 \Delta_h f'(\mathbf{c}) - M_0 \kappa \Delta_h^2 \mathbf{c} \tag{17}$$

where

$$\Delta_h f'(\mathbf{c}) = \frac{f'(\mathbf{c}_{i-1,j}) - 2f'(\mathbf{c}_{i,j}) + f'(\mathbf{c}_{i+1,j})}{h^2} + \frac{f'(\mathbf{c}_{i,j-1}) - 2f'(\mathbf{c}_{i,j}) + f'(\mathbf{c}_{i,j+1})}{h^2} \tag{18}$$

$$\Delta_h \mathbf{c} = \frac{\mathbf{c}_{i-1,j} - 2\mathbf{c}_{i,j} + \mathbf{c}_{i+1,j}}{h^2} + \frac{\mathbf{c}_{i,j-1} - 2\mathbf{c}_{i,j} + \mathbf{c}_{i,j+1}}{h^2} \tag{19}$$

$$\Delta_h^2 \mathbf{c} = \frac{\mathbf{c}_{i-2,j} - 4\mathbf{c}_{i-1,j} + 6\mathbf{c}_{i,j} - 4\mathbf{c}_{i+1,j} + \mathbf{c}_{i+2,j}}{h^4} + \frac{\mathbf{c}_{i,j-2} - 4\mathbf{c}_{i,j-1} + 6\mathbf{c}_{i,j} - 4\mathbf{c}_{i,j+1} + \mathbf{c}_{i,j+2}}{h^4} \tag{20}$$

We can perform a von Neumann stability analysis by linearizing $f'(\mathbf{c})$ around one of the equilibrium points $\mathbf{c} = \pm 1$. For simplicity lets analyze the 1D case. This will provide an approximation on the stability region of the various schemes. As per standard in von Neumann analysis, assume the solution takes the form $\mathbf{c}(\mathbf{x},t) = c_0 e^{ikx} e^{\Omega_r t} e^{i\Omega_i t}$. We substitute this into the 1D version of 17 and solve for $\Omega = \Omega_r + i\Omega_i$ leading to

$$\Omega = -\frac{8M_0}{h^2}\sin^2\left(\frac{kh}{2}\right) - \frac{16M_0\kappa}{h^4}\sin^4\left(\frac{kh}{2}\right) \tag{21}$$

where the first term is the expression for the linearized potential and second term for the homogeneous solution. Since M, κ are positive by definition, Ω is always negative

and meaning this discretization (linearizing our potential) is stable producing no periodic oscillations.

3.2 Temporal Discretization

3.2.1 Explicit One Stage RK Shceme - Forward Euler

The explicit one stage RK is equivalent to the Forward Euler (FE) scheme where we discretize the time derivative as

$$\frac{\partial \mathbf{c}}{\partial t} = \frac{\mathbf{c}_{ij}^{n+1} - \mathbf{c}_{ij}^{n}}{\Delta t} \tag{22}$$

The stability condition for the FE scheme is $(1 + \Omega_r \Delta t)^2 + \Omega_i^2 \Delta t^2 < 1$. Combined with the central FD scheme this leads to a stability condition of

$$\Omega_r \Delta t = -16C_1 \sin^4\left(\frac{kh}{2}\right) - 8C_2 \sin^2\left(\frac{kh}{2}\right) > -16C_1 - 8C_2 > -2 \tag{23}$$

$$2C_1 + C_2 < \frac{1}{4} \tag{24}$$

where we define the Courant numbers $C_1 = M_0 \kappa \frac{\Delta t}{h^4}$ and $C_2 = M_0 \frac{\Delta t}{h^2}$. Thus, as expected, this scheme is conditionally stable. Even looking at the homogenous equation and C_1, this scheme is expensive as doubling the spatial discretization requies the time step to be reduced by a factor of 16. A similar analysis can be performed in 2D which leads to a similarly conditionally stable, expensive scheme.

3.2.2 Explicit Four Stage RK Scheme - The Runge Kutta Method

The Runge Kutta Method is defined by the following temporal discretization as a butcher table

$$\begin{array}{c|cccc} 0 & & & & \\ \frac{1}{2} & \frac{1}{2} & & & \\ \frac{1}{2} & 0 & \frac{1}{2} & & \\ 1 & 0 & 0 & 1 & \\ \hline & \frac{1}{6} & \frac{1}{3} & \frac{1}{3} & \frac{1}{6} \end{array}$$

While this scheme provides more stability than the Forward Euler allowing for larger time steps, it is still conditionally stable and not symplectic for larger time steps due to its explicit nature. This will be explored more in the results section.

3.2.3 Implicit One Stage Runge Kutta Scheme

Explicit methods are often intractable due to severe restrictions on size of time step arising from the stiffness of the equation. This makes them computationally prohibitive even for

simple problems as seen above. Furthermore these schemes are generally unstable when using the non-linear form of the potential energy and not symplectic, leading to a lack of conservation of energy as seen in the 4 unless the time steps are extremely small. Thus implicit and semi-implicit schemes can provide L stability and flexibility in the size of the time steps.

The implicit one stage Runge Kutta scheme is the same as the backward euler scheme where

$$\frac{\partial \mathbf{c}^{n+1}}{\partial t} = \frac{\mathbf{c}_{ij}^{n+1} - \mathbf{c}_{ij}^{n}}{\Delta t}. \tag{25}$$

Due to the non-linearity, we linearize $f'(c)$ about an equilibrium point and use one Newton iteration of the Raphson-Newton iterative scheme to solve the non-linear equation. This implicit scheme is L-stable for large time steps which allows us to use adaptive time steps.

In the explicit Runge-Kutta themes, adaptive time steps would have led to instability in the numerical scheme. However a scheme allowing adaptive time steps is ideal due to the slow changes in the concentration during the coarsening part of the evolution. For the implicit schemes here and below, we use as simple tolerance ratio threshold of 0.01 between iterations where the time steps are doubled

3.2.4 Explicit Singular Diagonally Implicit RK (ESDIRK) Scheme

ESDIRK methods are designed in such a way that all stage weights coefficients are non zero only on the lower triangular matrix as shown in the following Butcher table. Due to this, the solving procedure for all stages can be successively separated in contrast to the implicit methods that require non-linear solvers for the full matrix. Instead, the same Jacobian matrix can be used for each stage to solve the non-linear equation of a reduce dimensional space. This method was explored for Navier-Stokes style PDEs in Bijl et al., 2002.

We will use a fourth order ESDIRK method that involves 6 stages. The following is the corresponding Butcher table

0	0	0	0	0	0	0
$\frac{1}{2}$	$\frac{1}{4}$	$\frac{1}{4}$	0	0	0	0
$\frac{83}{250}$	$\frac{8611}{62500}$	$-\frac{1743}{31250}$	$\frac{1}{4}$	0	0	0
$\frac{31}{50}$	$\frac{5012029}{34652500}$	$-\frac{654441}{2922500}$	$\frac{174375}{388108}$	$\frac{1}{4}$	0	0
$\frac{17}{20}$	$\frac{15267082809}{155376265600}$	$-\frac{71443401}{120774400}$	$\frac{730878875}{902184768}$	$\frac{2285395}{8070912}$	$\frac{1}{4}$	0
1	$\frac{82889}{524892}$	0	$\frac{15625}{83664}$	$\frac{69875}{102672}$	$-\frac{2260}{8211}$	$\frac{1}{4}$
	$\frac{82889}{524892}$	0	$\frac{15625}{83664}$	$\frac{69875}{102672}$	$-\frac{2260}{8211}$	$\frac{1}{4}$

Recall that for each stage we solve the intermediate non-linear problem

$$c_p = c^n + \Delta t \sum_{j=1}^{s} a_{pj} k_j \text{ for } p = 1, .., s \text{ with } k_p = \frac{\partial c_p}{\partial t} \tag{26}$$

with the final solution being

$$c_{n+1} = c^n + \Delta t \sum_{j=1}^{s} b_j k_j \tag{27}$$

This scheme, due to it being of fourth order and involving non-linear solvers, is more expensive than the previous schemes. However, this results in a better simulation over larger time scales compared to the other approaches. Unfortunately data was unable to be collected but it is still in the code base to review.

4. Numerical Results

We will start with a uniformly random initial condition centered at 0 defined by $c_0 = 0.05 * \text{random.uniform}(-1, 1)$:

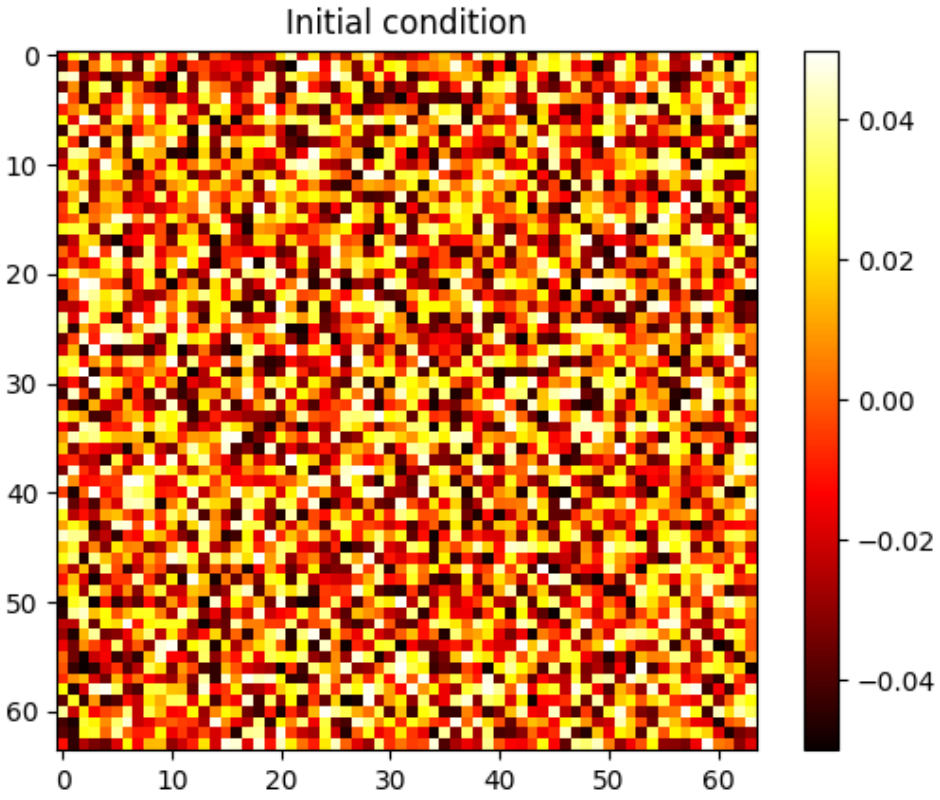

Figure 3: The initial concentration of a uniformly random distribution between -0.05 and 0.05

We will limit the number of iterations any scheme can perform to 1000 or the final time be 0.1 seconds. Figure (4) demonstrates how the systems energy changes over time for each scheme.

Looking into each scheme specifically we have the following evolution

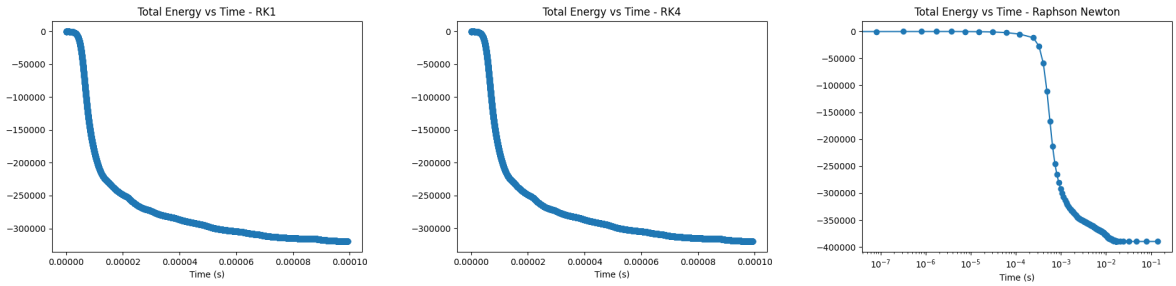

Figure 4: Demonstrates the decreasing energy of the system for explicit RK1 (left), explicit RK4 (middle) and implicit RK1 (right). Notice the time scales are different because each simulation only had a max iteration of 1000. The implicit method is able to cover a larger time scale with same iteration count

4.1 One Stage Explicit Runge-Kutta - Forward Euler

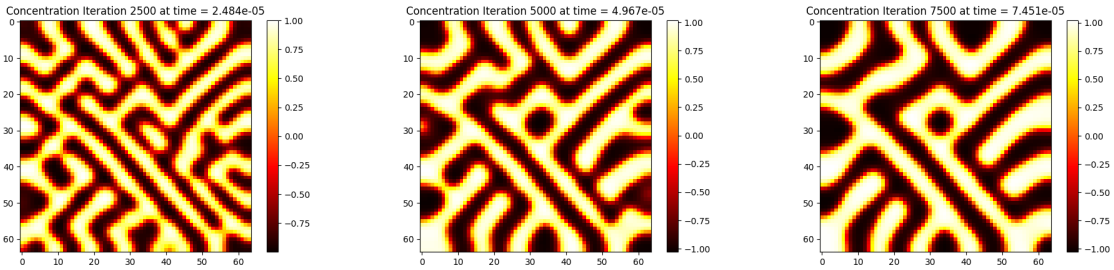

Figure 5: Evolution over 7500 iterations. Due to the small time step, it only covers about one order of magnitude of time. Concentrations rich in one component are bright(+1) and concentrations rich in the other component are dark (-1).

4.2 Four Stage Explicit Runge-Kutta - The Runge-Kutta Method

4.3 One Stage Implicit Runge-Kutta - Backward Euler

5. Methodology for Expanding Complexity of Cahn-Hillard Equation

Some of the main extensions of the Cahn-Hillard equation are the following: analyzing the quenching process by making the free energy per molecule function $f(\mathbf{c})$ time dependent, modifying the domain by replacing periodic boundary conditions to fixed ones and modifying the geometry of the domain, expand the simulation from 2D to 3D, and analyze ternary systems. The field continues to look at various numerical ways to approaching these various adaptations, using the strengths of each numerical scheme to match the bias of the problem. For instance, time adaptive and thus (semi) implicit schemes are useful for modeling a time-dependent $f(\mathbf{c})$ where there will be oscillations between fast phase separation and slow coarsening. Furthermore for complex geometries with new boundary

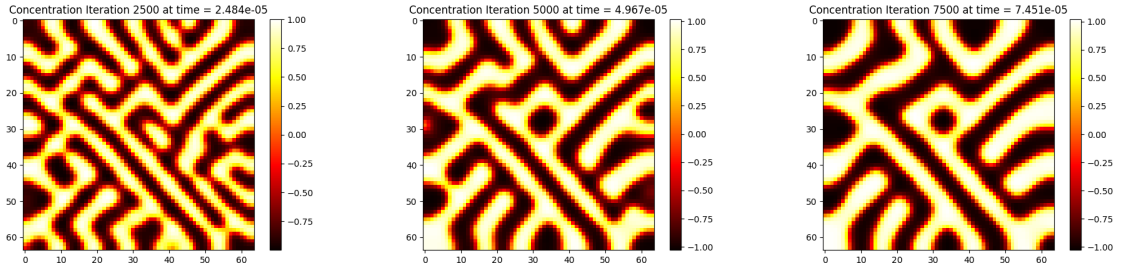

Figure 6: Evolution over 7500 iterations. Due to the small time step, it only covers about one order of magnitude of time. Concentrations rich in one component are bright(+1) and concentrations rich in the other component are dark (-1). Stability is increased allowing for slightly larger time steps.

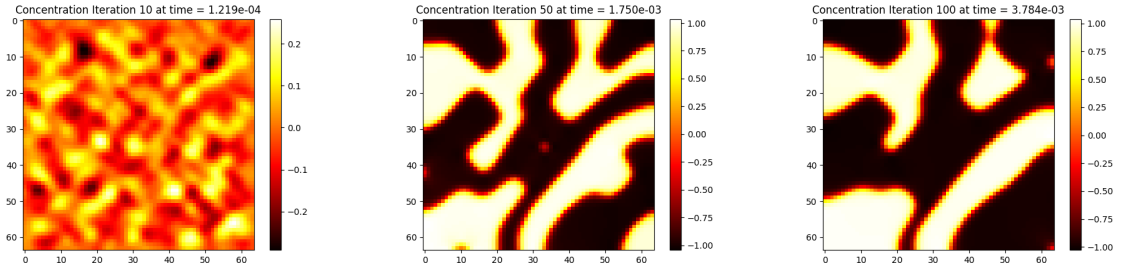

Figure 7: Evolution over 100 iterations. Due to the adaptive time step, it covers about three orders of magnitude of time in only 100 iterations. With this scheme more of the dynamics are visible. Concentrations rich in one component are bright(+1) and concentrations rich in the other component are dark (-1).

conditions a more robust spatial discretization such as a Galerkin finite element would be preferable since the dynamics are space dependent.

6. Conclusion

The Cahn-Hillard equation is a difficult non-linear PDE to simulate even for a simplified case due to its stiffness, drastically vary time and space dynamics, and non-linearity. However, using the family of Runge-Kutta methods already provides strong methods to simulate the dynamics. Understanding the fundamentals of the Cahn-Hillard equation, such as its decreasing total energy and difference in time scale dynamics, provides intuition on why to use time adaptive and symplectic Runge-Kutta schemes.

The explicit Runge-Kutta schemes are quick to calculate requiring no non-linear solvers or linearizations of the energy functional. However due to the fourth order derivative and conditional stability, they are restricted to small time steps making it difficult to simulate long time dynamics. The implicit Runge-Kutta schemes are more costly, requiring non-linear solvers making each stage computationally more expensive. This particularly is an issue as you increase the mesh size as the matrix grows exponentially. However, due to their L-stability, we can add time adaptivity - taking small time steps for the quick phase

separation and large time steps for the coarsening process. Since the majority of the time the dynamics are undergoing coarsening, this significantly reduces the overall compute time. Finally, we can take the benefits of both schemes with an ESDIRK scheme that inherits the L-stability properties of the implicit scheme but reduces the dimensionally of the inversion process by decoupling the equations and using the same LU decomposition matrix as all stages.

References

Amiri, F., Ziaei-Rad, S., Valizadeh, N., & Rabczuk, T. (2019). On the use of local maximum entropy approximants for cahn-hilliard phase-field models in 2d domains and on surfaces. *Computer Methods in Applied Mechanics and Engineering*, 346, 1–24.

Bijl, H., Carpenter, M. H., Vatsa, V. N., & Kennedy, C. A. (2002). Implicit time integration schemes for the unsteady compressible navier–stokes equations: Laminar flow. *Journal of Computational Physics*, 179(1), 313–329.

Shin, J., Choi, Y., & Kim, J. (2019). The cahn–hilliard equation with generalized mobilities in complex geometries. *Mathematical Problems in Engineering*, 2019, 1710270. https://doi.org/10.1155/2019/1710270

Valizadeh, N., & Rabczuk, T. (2019). Isogeometric analysis for phase-field models of geometric pdes and high-order pdes on stationary and evolving surfaces. *Computer Methods in Applied Mechanics and Engineering*, 351, 599–642.

Zimmermann, C., Toshniwal, D., Landis, C. M., Hughes, T. J., Mandadapu, K. K., & Sauer, R. A. (2019). An isogeometric finite element formulation for phase transitions on deforming surfaces. *Computer Methods in Applied Mechanics and Engineering*, 351, 441–477.